Plasmon mass scale in two-dimensional classical nonequilibrium gauge theory

Lappi, T.

2018-02-15

Lappi , T & Peuron , J 2018 , ' Plasmon mass scale in two-dimensional classical nonequilibrium gauge theory ' , Physical Review D , vol. 97 , no. 3 , 034017 . https://doi.org/10.1103/PhysRevD.97.03

http://hdl.handle.net/10138/251196
https://doi.org/10.1103/PhysRevD.97.034017

Plasmon mass scale in two-dimensional classical nonequilibrium gauge theory

T. Lappi*
Department of Physics, P.O. Box 35, 40014 University of Jyväskylä, Finland
and Helsinki Institute of Physics, P.O. Box 64, 00014 University of Helsinki, Finland

J. Peuron
Department of Physics, P.O. Box 35, 40014 University of Jyväskylä, Finland

(Received 12 December 2017; published 15 February 2018)

We study the plasmon mass scale in classical gluodynamics in a two-dimensional configuration that mimics the boost-invariant initial color fields in a heavy-ion collision. We numerically measure the plasmon mass scale using three different methods: a hard thermal loop (HTL) expression involving the quasiparticle spectrum constructed from Coulomb gauge field correlators, an effective dispersion relation, and the measurement of oscillations between electric and magnetic energies after introducing a spatially uniform perturbation to the electric field. We find that the HTL expression and the uniform electric field measurement are in rough agreement. The effective dispersion relation agrees with other methods within a factor of 2. We also study the dependence on time and occupation number, observing similar trends as in three spatial dimensions, where a power-law dependence sets in after an occupation-number-dependent transient time. We observe a decrease of the plasmon mass squared as $t^{-1/3}$ at late times.

DOI: 10.1103/PhysRevD.97.034017

I. INTRODUCTION

The color glass condensate (CGC) [1,2] is an effective theory of quantum chromodynamics (QCD) at high energy. One of the remarkable predictions of CGC is that two colliding CGC sheets create gluon states with nonperturbatively high occupation numbers $1/g^2$ [3], which can be described using classical fields [4].

The question of how this strongly interacting matter eventually isotropizes and thermalizes has been a longstanding question in the theory of ultrarelativistic heavy-ion collisions. According to our current understanding, the classical picture is valid for a short time after the initial collision, until the occupation numbers fall below unity. The out-of-equilibrium matter admits a kinetic theory description when the occupation numbers are $1/g^2$. Fortunately, the kinetic theory description also has an overlapping range of validity with classical simulations [5–7], meaning that the two can be smoothly matched. In recent simulations the equilibration process has been studied by matching kinetic theory and relativistic hydrodynamics with promising results [8].

Calculations in the high collision energy limit, using the CGC formalism, predict that the initial color field configurations are boost invariant to leading order in the coupling [9–13]. In practice the longitudinal structure of the colliding nuclei breaks this boost invariance at finite collision energies [14–16]. In this paper we are, however, interested in the case where the boost invariance is only broken by small quantum fluctuations [17–21]. Due to instabilities, which are present in non-Abelian plasma [22–38], even very small violations of boost invariance can grow rapidly and become comparable to the classical background field. The plasma instability growth rate is determined by the plasmon mass scale [39,40], and therefore, studying the plasmon mass can also shed light on the issue of isotropization and thermalization of plasma in ultrarelativistic heavy-ion collisions.

The aim of this paper is to compare different methods to estimate the plasmon mass in classical Yang-Mills systems in the case where a three-dimensional theory exists in a two-dimensional configuration. In practice we implement this by using a three-dimensional calculation on a lattice with only one point in the z direction. This configuration mimics the very anisotropic, nearly boost-invariant, field

*tuomas.v.v.lappi@jyu.fi
jarkko.t.peuron@student.jyu.fi

configuration predicted by the CGC for the initial stage of a heavy-ion collision. At this stage we neglect the longitudinal expansion of the system in a heavy-ion collision and work on a fixed size lattice. Instead of calculating in the asymptotically large time regime, where a clear separation between the hard and Debye scales has developed, we also want to address relatively early times where it is less obvious that such a scale separation exists. At this regime of earlier times one can also study the dependence on the parameters of the initial condition, the occupation number, and the hard scale, separately.

To extract the plasmon mass we will systematically compare three methods, which we already compared in three dimensions [41]. The first method will be to use a formula one can derive in hard thermal loop (HTL) perturbation theory. Even though the HTL-like scale separation is not guaranteed by the weak coupling in the classical theory, the plasmon mass scale nevertheless exists [39,40,42–44]. The second method involves perturbing the system with a spatially uniform electric field (UEF) [45] and measuring the response to this zero momentum perturbation. The third method involves the effective dispersion relation (DR) [42], which we can extract from the Coulomb gauge correlators of the fields.

The HTL formula relies on the quasiparticle spectrum, which is also typically extracted from Coulomb gauge correlators of the classical fields. However, we will notice that at high occupation numbers in two spatial dimensions the gauge fixing has a deforming effect on the observed quasiparticle spectrum. Thus, we will argue for the need to use gauge-invariant observables for measuring the typical momentum scale and occupation number.

We will first briefly introduce the numerical methods and initial conditions in Sec. II. In Sec. III we will introduce the three methods we use to extract the plasmon mass. Then we move on to dependencies on the lattice cutoffs, time, and occupation number in Sec. IV. Finally, we conclude in Sec. V.

II. NUMERICAL METHOD AND INITIAL CONDITIONS

A. Equations of motion in the temporal gauge

We have done all the numerical simulations with the SU(2) gauge group for numerical convenience. Several studies have compared SU(2) and SU(3) gauge groups, demonstrating qualitatively similar results [46–48]. We use the standard pure gauge Wilson action on a three-dimensional lattice

$$S = \sum_{x,i} \frac{1}{N}\mathrm{ReTr}\left(1 - U^{0;i}_x\right) + \sum_{x,i<j} \frac{1}{N}\mathrm{ReTr}\left(1 - U^{i;j}_x\right), \quad (1)$$

where $\beta_0 = \frac{2N}{g^2}$, $\beta_s = \frac{2N}{g^2}$, $\gamma = \frac{a_s}{a_t}$, N is the number of colors and $U_{x,i}$ are the link matrices defined as

$$U_{x,i} = \exp(i a_s g A_i(x)). \quad (2)$$

The plaquette variables appearing in (1) are defined as $U^{i;j}_x = U_{x,i} U_{x+\hat{i},j} U^\dagger_{x+\hat{j},i} U^\dagger_{x,j}$. The spatial lattice spacing is a_s, and the time step is denoted by a_t. We use standard normalization for the SU(2) generators, $\mathrm{Tr}(t^a t^b) = \frac{1}{2}\delta^{ab}$. The relationships between the lattice variables and the actual fields are given by the following equations:

$$E^a_i(x) = \frac{2}{a_s a_t g}\mathrm{ImTr}\left(t^a U^{i;0}_x\right), \quad (3)$$

$$B^a_i(x) = \frac{\epsilon^{ijk}}{a_s^2 g}\mathrm{ImTr}\left(t^a U^{j;k}_x\right), \quad (4)$$

$$F^a(x) = \frac{2}{a\,a\,g}\mathrm{ImTr}\left(t^a U^{;}_x\right), \quad (5)$$

$$A^a(x) = \frac{2}{a\,g}\mathrm{ImTr}\left(t^a U_{x;}\right). \quad (6)$$

We refer to the lattice spacing in the i direction with a_i. The equations of motion of the electric field are obtained by varying the action (1) with respect to the spatial links

$$E_j(t; x) = E_j(t - a_t; x) + \frac{a_t}{2i a_s^3 g}\sum_k \left(U^{j;k}_x - U^{k;j}_x\right) + \frac{1}{N}\mathrm{Tr}\left(U^{j;k}_x - U^{k;j}_x\right)\left(\bar{U}^{j;k}_x - \left(\bar{U}^{j;k}_x\right)^\dagger\right) - \frac{1}{N}\mathrm{Tr}\left(\bar{U}^{j;k}_x - \left(\bar{U}^{j;k}_x\right)^\dagger\right), \quad (7)$$

where $\bar{U}^{j;k}_x = U_{x,j} U_{x+\hat{j},k} U^\dagger_{x+\hat{k},j} U^\dagger_{x,k}$. When the electric field on the next time step is known, we can easily construct the temporal plaquette [when using the SU(2) symmetry group] by decomposing the temporal plaquette into two parts:

$$U^{i;0}_x = \sqrt{1 - \frac{a_s a_t g}{2}E_a^2}\,\mathbb{1} + i a_s a_t g E^a t^a. \quad (8)$$

In the temporal gauge the temporal plaquette simplifies to a product of link matrices at two different time steps, making it easy to solve for the link at the next time step. Color charge conservation is encoded in Gauss's law,

$$\sum_j \left(E_j(x) - U_{x-\hat{j},j} E_j(x - \hat{j}) U^\dagger_{x-\hat{j},j}\right) = 0, \quad (9)$$

which is preserved by the discretization algorithm.

B. Quasiparticle distribution

We extract the quasiparticle spectrum by eliminating the residual gauge freedom with the Coulomb gauge condition. The gauge fixing is done by a Fourier accelerated algorithm [49]. However, even with gauge fixing, there is no unique way to determine a quasiparticle distribution from a given classical field configuration (see also the discussion in Refs. [45,50]). If our system can be described by weakly interacting quasiparticles, the energy density of the system should be obtained as

$$\ldots 2\left(N_c^2 - 1\right) \int \frac{d^3k}{(2\pi)^3} \omega(k) f(k). \tag{10}$$

Here the factor $2(N_c^2 - 1)$ accounts for the number of color and transverse polarization states in the system. The number of physical polarization states the plasmons have is 3. However, the longitudinal mode is only present for modes close to the Debye scale and is not expected to contribute significantly to the total energy density (10). Thus a factor 3 would lead to a significant underestimation of the occupation number of hard modes. The total energy of the system is given by the Hamiltonian

$$H = \int d^3x \mathrm{Tr}\left(E_i E^i + B_i B^i\right). \tag{11}$$

We now keep only the terms which are quadratic in the gluon field and equate the energy given by the Hamiltonian with the one given by the quasiparticle spectrum. Solving for the quasiparticle spectrum gives

$$f_{A+E}(k) = \frac{1}{4(N_c^2 - 1)V} \frac{|E_C(k)|^2}{\omega(k)} + \frac{k^2}{\omega(k)} |A_C(k)|^2 \,. \tag{12}$$

Here $|E_C(k)|$ is the Coulomb gauge electric field and $|A_C(k)|$ is the gauge field in Coulomb gauge. This procedure also removes the magnetic part of the longitudinal polarization state. The energy of a mode with momentum k (the dispersion relation) is given by $\omega(k)$. When extracting the quasiparticle spectrum we will assume a massless dispersion relation $\omega(k) = k$. It is not immediately obvious what would be the correct procedure to self-consistently include a plasmon mass in the dispersion relation used here. In any case the effect of such a correction would be of the same order as the higher order terms in the gauge potential that we are already neglecting in Eq. (12).

Alternatively, we can also extract the quasiparticle spectrum using only the gauge fields, or only electric fields. These two should be equivalent above the Debye scale after the system has been evolved in time for a few Q^{-1}. The alternative definitions for the occupation number are

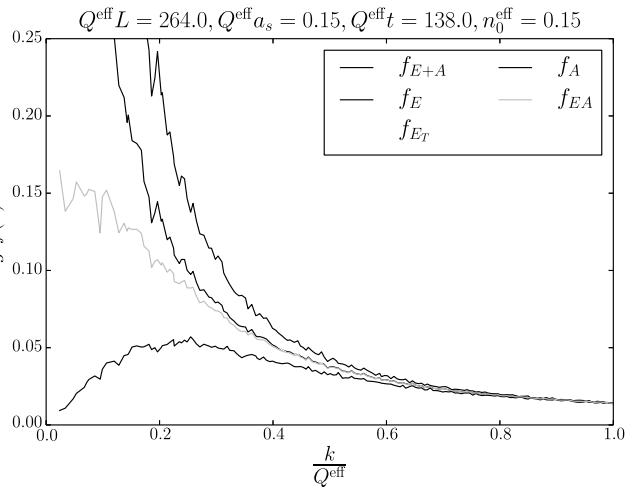

FIG. 1. Occupation number extracted using different methods. Averaged over 20 configurations.

$$f_E(k) = \frac{1}{2(N_c^2 - 1)} \frac{1}{(1/V)} \frac{|E_C(k)|^2}{\omega(k)} \tag{13}$$

for the electric estimator and

$$f_A(k) = \frac{1}{2(N_c^2 - 1)} \frac{1}{(1/V)} \frac{k^2}{\omega(k)} |A_C(k)|^2 \tag{14}$$

for the magnetic estimator. We can also use a combination of electric and magnetic fields,

$$f_{EA}(k) = \frac{1}{2(N_c^2 - 1)} \frac{1}{(1/V)} \sqrt{|A_C(k)|^2 |E_C(k)|^2} \,. \tag{15}$$

We compare these different definitions for the occupation number in Fig. 1. We observe that the electric occupation number diverges in the infrared, whereas the magnetic estimator is IR finite. The combination of electric and magnetic fields $f_{(EA)}$ also behaves reasonably well in the IR. This behavior is to be expected since below the Debye scale we would not expect the dispersion relation to be massless. We will return to this question later in the context of using these distributions. Figure 1 also demonstrates the transverse electric occupation number. We clearly see that it is very close to the total electric occupation number, especially at higher momenta, indicating that the quasiparticle spectrum is dominated by transverse plasmons.

C. Initial conditions

The initial gauge fields are sampled from the distribution

$$\langle A_i^a(k) A_j^b(p) \rangle = \frac{V n_0}{g^2 Q} \exp\left(-\frac{k^2}{Q^2}\right) \delta_{ij} \delta^{ab} \frac{(2\pi)^3 \delta(k + p)}{V}. \tag{16}$$

Since our system is two dimensional, the z components of the momenta are in fact always zero, and the exponential is $\exp(-k^2/Q^2) = \exp(-k^2/Q^2)$. Here Q is the dominant momentum scale, V is the lattice volume, and n_0 is a parameter describing the typical occupation number of the system. This initial condition is a momentum distribution clearly peaked around Q, and it behaves very well in the ultraviolet and infrared regions. It also trivially satisfies Gauss's law since it contains only magnetic energy. In the context of the early stages of heavy-ion collisions, we should consider Q as analogous to the saturation scale Q_s [51]. For the classical approximation to be valid, the occupation number $f = n_0/g^2$ should be greater than of the order of 1, i.e., $n_0 \gg g^2$.

Our choice of initial fields, using (12) as the quasiparticle distribution, results in the following form,[1]

$$f(k, t = 0) = \frac{n_0}{2g^2}\frac{k}{Q}\exp\left(-\frac{k^2}{2Q^2}\right)(2\pi)(k_z). \quad (17)$$

where a_s is the length of the system in the z direction.

We are using the same initial condition as in Refs. [52,53]. This distribution is strongly cut off in the UV and is, in this regard, similar to initial conditions used in Refs. [54,55]. For more realistic initial conditions we refer the reader to, for example, Refs. [56,57]. The precise functional form of the initial condition does not very strongly affect the late-time behavior of the system (unless one changes the occupation number by a very large margin) because overoccupied classical Yang-Mills systems eventually evolve into a well-known scaling solution in a time of the order of a few Q/t [45,54,58]. Similar findings have also been made in scalar field theories [55,59,60].

D. Measured observables

Our initial condition (16) is constructed with the gauge fields in momentum space. These are then Fourier transformed back to coordinate space and exponentiated to form the link matrices that are the actual variables in the calculation. In order to measure the quasiparticle spectrum (12), one then fixes the Coulomb gauge and calculates the anti-Hermitian traceless part of the link matrix to get the gauge potential A_i appearing in the expression (12). This process is very nonlinear, and in the high density regime it is not obvious that one recovers the same quasiparticle distribution that one put in as an initial condition. In order to control the limits in this process, it is useful to compare

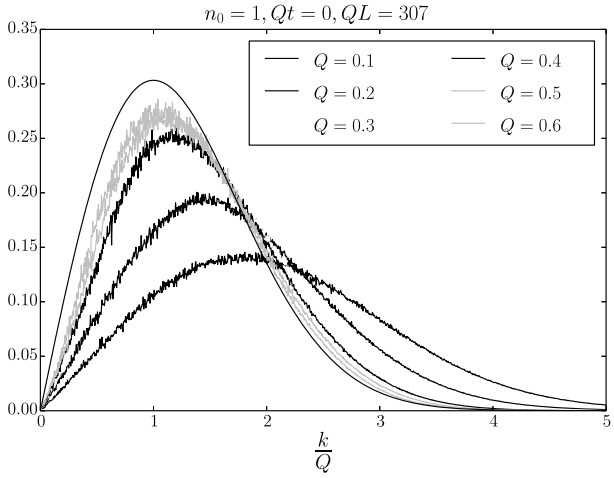

FIG. 2. The effect of the initial momentum scale on the observed quasiparticle spectrum. The configurations which are closest to the continuum deviate the most from the analytical form (17) used as an input, shown as the smooth black line. Averaged over 10 runs.

the measured quasiparticle distribution at $t = 0$ to the one used in the initial condition. This comparison is shown in Figs. 2 and 3. Figure 2 shows the dependence of the gauge-fixed quasiparticle spectrum on the initial momentum scale. We observe that the gauge-fixed spectrum deviates the most from the analytical initial condition when Q/a_s is small. Figure 3 shows the gauge-fixed spectrum for different occupation numbers. Here we find a similar effect: at higher occupancy the gauge fixing significantly drives the spectrum away from the analytical initial condition by redistributing the energy to higher momentum modes and